THE JOURNAL OF BIOLOGICAL CHEMISTRY VOL. 284, NO. 7, pp. 4484–4493, February 13, 2009

Loop Gating of Connexin Hemichannels Involves Movement of Pore-lining Residues in the First Extracellular Loop Domain*

Received for publication, September 25, 2008, and in revised form, December 4, 2008 Published, JBC Papers in Press, December 11, 2008, DOI 10.1074/jbc.M807430200

Vytas K. Verselis[‡1], Maria P. Trelles[§], Clio Rubinos[§], Thaddeus A. Bargiello[‡], and Miduturu Srinivas[§2]

From the [‡]Department of Neuroscience, Albert Einstein College of Medicine, Bronx, New York 10461 and the [§]Department of Biological Sciences, State University of New York, State College of Optometry, New York, New York 10036

Unapposed connexin hemichannels exhibit robust closure in response to membrane hyperpolarization and extracellular calcium. This form of gating, termed "loop gating," is largely responsible for regulating hemichannel opening, thereby preventing cell damage through excessive flux of ions and metabolites. The molecular components and structural rearrangements underlying loop gating remain unknown. Here, using cysteine mutagenesis in Cx50, we demonstrate that residues at the TM1/E1 border undergo movement during loop gating. Replacement of Phe[43] in Cx50 with a cysteine resulted in small or no appreciable membrane currents. Bath application of dithiothreitol or TPEN (*N*,*N*,*N*′,*N*′-tetrakis(2-pyridylmethyl) ethylenediamine), reagents that exhibit strong transition metal chelating activity, led to robust currents indicating that the F43C substitution impaired hemichannel function, producing "lock-up" in a closed or poorly functional state due to formation of metal bridges. In support, Cd^{2+} at submicromolar concentrations (50–100 nM) enhanced lock-up of F43C hemichannels. Moreover, lock-up occurred under conditions that favored closure, indicating that the sulfhydryl groups come close enough to each other or to other residues to coordinate metal ions with high affinity. In addition to F43C, metal binding was also found for G46C, and to a lesser extent, D51C substitutions, positions found to be pore-lining in the open state using the substituted-cysteine accessibility method, but not for A40C and A41C substitutions, which were not found to reside in the open pore. These results indicate that metal ions access the cysteine side chains through the open pore and that closure of the loop gate involves movement of the TM1/E1 region that results in local narrowing of the large aqueous connexin pore.

Connexins are a large family of homologous integral membrane proteins that form gap junction (intercellular) channels that provide a direct communication pathway between neighboring cells. Gap junctions are formed by the docking of two hemichannels, which themselves can function in an undocked or unapposed configuration as ion channels that signal across the plasma membrane. Each hemichannel is composed of a hexamer of connexin subunits. The accepted membrane topology of a connexin subunit has four transmembrane domains (TM1–TM4)[3] and two extracellular loops (E1 and E2) with amino and carboxyl termini located intracellularly (reviewed in Ref. 1).

Connexin cell-cell channels and hemichannels are voltage dependent and two distinct voltage-sensitive gating mechanisms appear to be built into each hemichannel (2). One gating mechanism proposed to be located at the cytoplasmic end of the hemichannel is termed V_j gating, a name derived from studies of gap junction (cell-cell) channels describing sensitivity to transjunctional voltage, V_j, the voltage difference between coupled cells. The other gating mechanism is putatively ascribed to the extracellular end of the hemichannel and has been provisionally termed loop gating, because of the resemblance of gating transitions to those associated with initial opening of newly formed cell-cell channels (3, 4), a process that conceivably involves the extracellular loop domains.

Loop gating is a robust gating mechanism that together with extracellular divalent cations, principally Ca^{2+}, is largely responsible for keeping unapposed hemichannels closed at resting membrane potentials (5). Reports have suggested that extracellular divalent cations act as gating particles that enter and block the pore upon hyperpolarization (6, 7). An alternative model was recently proposed whereby extracellular divalent cations act as modulators of loop gating, an intrinsically voltage-sensitive mechanism, by stabilizing the closed conformation and shifting activation such that opening occurs at more positive potentials (8).

Although loop gating plausibly involves conformational changes associated with the extracellular loops, molecular components underlying loop gating as well as the location of the putative gate remain unknown. A recent study using chick homologues to the mammalian connexins, Cx46 and Cx50, reported that two charged residues were important determi-

* This work was supported, in whole or in part, by National Institutes of Health Grants GM54179 (to V. K. V.) and EY13869 (to M. S.). The costs of publication of this article were defrayed in part by the payment of page charges. This article must therefore be hereby marked "*advertisement*" in accordance with 18 U.S.C. Section 1734 solely to indicate this fact.

[1] To whom correspondence may be addressed: 1300 Morris Park Ave., Bronx, NY 10461. Tel.: 718-430-3680; Fax: 718-430-8944; E-mail: verselis@aecom.yu.edu.

[2] To whom correspondence may be addressed: SUNY, State College of Optometry, 33 West 42nd St., New York, NY 10036. Tel.: 212-938-5571; Fax: 212-938-5794; E-mail: msrinivas@sunyopt.edu.

[3] The abbreviations used are: TM, transmembrane; MTS-ET$^+$, 2-trimethylammonioethyl-methanethiosulfonate; MTSEA-biotin, 2-((biotinoyl)amino)-ethyl methanethiosulfonate); MTSEA-biotin-X, 2-((6-((biotinoyl)amino)-hexanoyl)amino)ethyl methanethiosulfonate); SCAM, substituted-cysteine accessibility method; WT, wild type; DTT, dithiothreitol; TPEN, *N*,*N*,*N*′,*N*′-tetrakis(2-pyridylmethyl)ethylenediamine; Cx, connexin.

nants of the different gating characteristics exhibited by these two connexin hemichannels (9). The implicated residues are at position 9 located in the NH_2-terminal domain and position 43 in the E1 domain. In Cx46 hemichannels, Glu^{43} and other flanking residues at the TM1/E1 border (Ala^{39}, Gly^{46}, and Asp^{51}) were shown to reside in the aqueous pore in the open state (10). Because it is likely that domains involved in permeation and gating of connexin channels are closely linked (reviewed in Ref. 11), we examined whether these residues are involved in structural rearrangements associated with loop gating. In this study, we engineered cysteines at residues in the TM1/E1 border in Cx50 hemichannels and used the ability of sulfhydryl groups to form disulfide bonds and/or to complex with heavy metal ions to report conformational changes that occur during gating.

EXPERIMENTAL PROCEDURES

Reagents—The MTS reagent MTS-ET^+ (2-trimethylammonioethyl-methanethiosulfonate) was purchased from Anatrace Inc. (Maumee, OH). MTSEA-biotin (2-((biotinoyl)amino)ethyl methanethiosulfonate) and MTSEA-biotin-X (2-((6-((biotinoyl)amino)hexanoyl)amino)ethyl methanethiosulfonate)) were purchased from Biotium, Inc. (Hayward, CA). Aliquots of dry powder were prepared and stored in microcentrifuge tubes at −20 °C. Prior to each experiment aliquots of MTS-ET^+ and MTSEA-biotin(-X) were dissolved in distilled water and dimethyl sulfoxide, respectively, chilled on ice, to a stock concentration of 250 mM. Dilutions were made into IPS just before application to the desired final concentration (ranging from 0.25 to 5 mM). Activity of MTS reagents were periodically checked using a 2-nitro-5-thiobenzoic acid assay (12). All other chemicals were purchased from Sigma.

Expression of Cx46 and Cx50 in Xenopus Oocytes—Cx46 DNA was cloned from rat genomic DNA using PCR amplification with primers corresponding to NH_2- and COOH-terminal sequences as described previously (5). The Cx50 coding sequence was subcloned into the SP64T transcription vector (kindly provided by Dr. Thomas White, SUNY, Stony Brook, NY). Synthesis of RNA and preparation and injection of oocytes have been described previously (5). Injected oocytes were kept at 18 °C in a modified ND96 solution containing (in mM) 88 NaCl, 1 KCl, 1 $MgCl_2$, 1.8 $CaCl_2$, 5 glucose, 5 HEPES, 5 pyruvate, pH 7.6. Site-directed mutagenesis was performed with QuikChange mutagenesis kit (Stratagene, La Jolla, CA) in accordance with the manufacturer's protocol using the wild-type connexin expression constructs as templates. All constructs were verified by sequencing.

Electrophysiological Recordings—To record macroscopic hemichannel currents, *Xenopus* oocytes were placed in a polycarbonate RC-1Z recording chamber (Warner Instruments, Hamden, CT) with a slot-shaped bath connecting inflow and outflow compartments to allow for rapid perfusion. A suction tube was placed in the outflow compartment and a separate reservoir was used for grounding, connected to the main chamber with an agar bridge. Bath volume was ~0.3 ml and total volume exchange was achieved in 5–10 s by application of solutions to the inflow compartment. Flow rates in all experiments were constant. At the start of each experiment, oocytes were bathed in the modified ND96 solution. Perfusion solutions con-

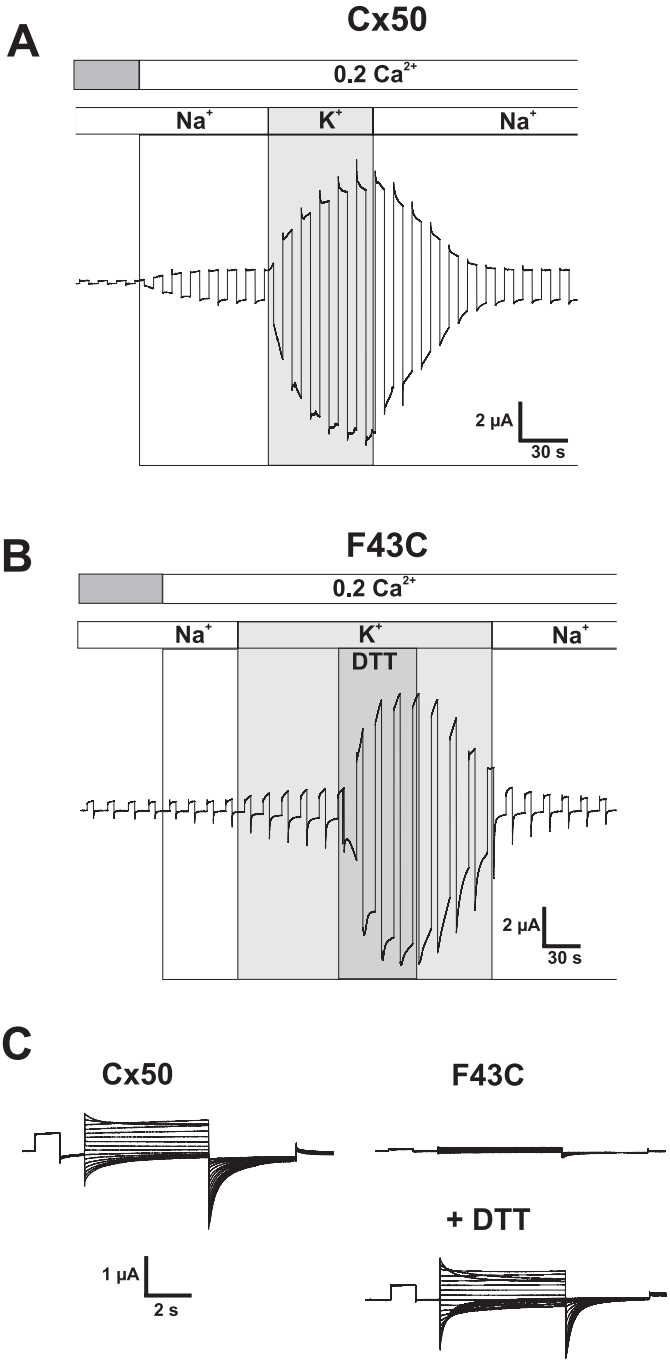

FIGURE 1. **F43C hemichannels exhibit impaired function, which is reversed by DTT.** *A*, macroscopic currents in oocytes expressing Cx50 in response to voltage steps to +40 mV applied from a holding potential of −40 mV. Reduction of external Ca^{2+} from 1.8 to 0.2 mM in a NaCl solution promoted opening of Cx50 hemichannels evident by the development of a current. Equimolar replacement of external Na^+ with K^+ in the continued presence of 0.2 mM Ca^{2+} caused a further and robust increase in the amplitude of the current (16). *B*, in contrast, currents in F43C-expressing oocytes showed no increase when Ca^{2+} was reduced, and replacement of Na^+ with K^+ produced only a modest increase in current magnitude indicating impaired function. Application of DTT (100 µM) rescued hemichannel function, suggesting disruption of disulfide bonds and/or metal binding. *C*, macroscopic currents in response to voltage steps from +60 to −110 mV in increments of 10 mV were applied from a holding potential of −20 mV. Currents in F43C-expressing oocyte in the presence of DTT are similar to those in oocytes expressing Cx50 showing reductions in conductance at both positive and negative voltages. In the absence of DTT, F43C channels showed no evidence of activation even at positive voltages.

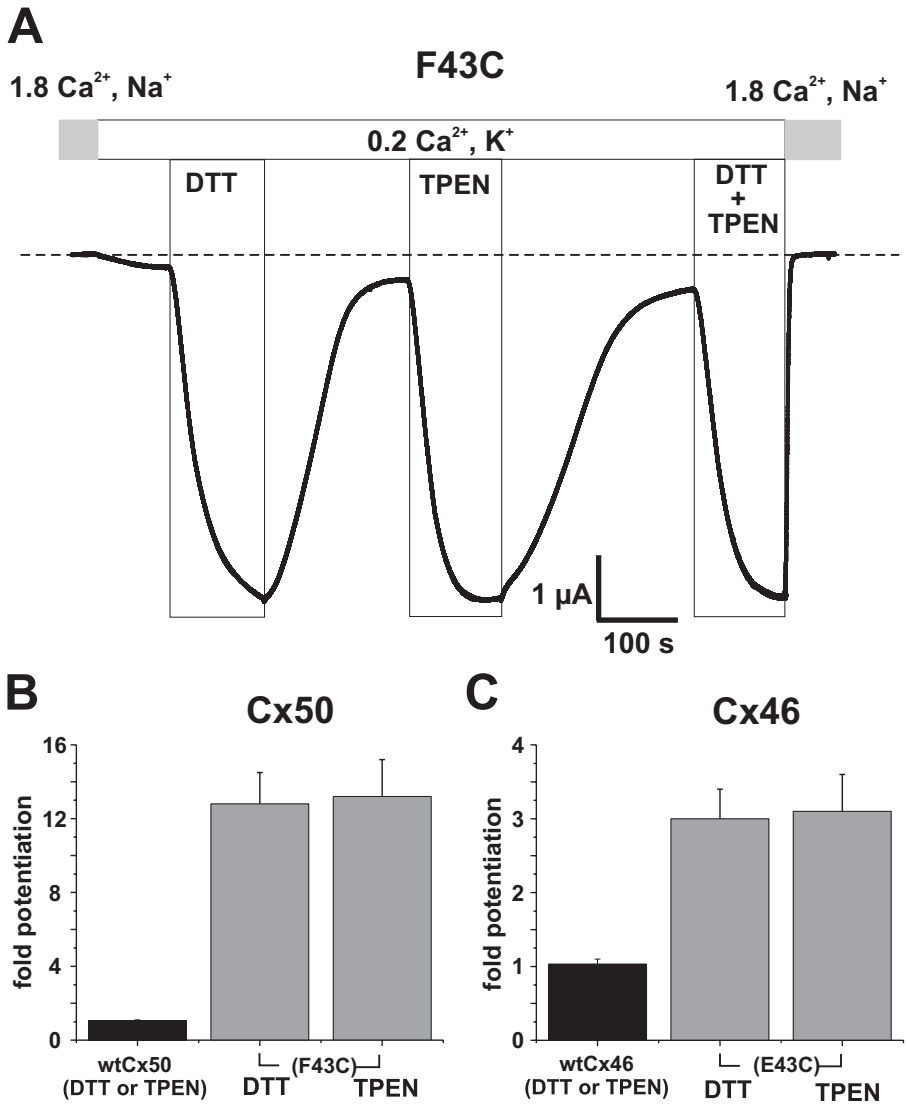

FIGURE 2. **Impaired function of F43C hemichannels is due to metal ion binding.** *A*, shown are membrane currents in a F43C-expressing oocyte voltage clamped at −40 mV. Application of DTT (100 μM) or TPEN (10 μM), effective chelators of transition metal ions, caused large reversible increases in current amplitude. Potentiation of current caused by TPEN and DTT was similar in magnitude, and the effects of TPEN and DTT when applied together were not additive, indicating that impaired function is due to formation of metal bridges with the introduced cysteine. *B*, *bar graph* summarizing the effects of TPEN ($n = 16$) and DTT ($n = 18$) on F43C channels (*left panel*). Cx50 WT channels are not affected by TPEN or DTT ($n = 12$; *solid bars*). *C*, both TPEN and DTT also increased current magnitude in oocytes expressing Cx46 hemichannels in which the glutamic acid at position 43 was replaced with cysteine (*i.e.* E43C, *right column*). Because Cx46 activates only at positive voltages, current amplitudes were measured at the ends of 5-s depolarizing voltage steps to +40 mV. Mean current values after DTT ($n = 6$) and TPEN ($n = 6$) were again similar. *Bars* represent the mean ± S.E. of the fold-change caused by each chelator.

sisted of (in mM) 100 NaCl or 100 KCl, 1 $MgCl_2$, and 10 HEPES, pH 8.0. $CaCl_2$ was added to adjust the Ca^{2+} concentration to the desired levels. In some experiments, solutions were prepared in water pre-treated with Calcium Sponge S (Invitrogen) to remove contaminating metals using salts containing low amounts of metallic impurities (Sigma). All recordings were obtained with a GeneClamp 500 two-electrode voltage clamp (Axon Instruments, Union City, CA). Both current-passing and voltage-recording pipettes contained 1 M KCl.

To record single hemichannel currents, *Xenopus* oocytes were manually devitellinized in a hypertonic solution consisting of (in mM) 220 sodium aspartate, 10 KCl, 2 $MgCl_2$, 10 HEPES, pH 7.6, and then placed in ND96 solution for recovery. Oocytes were moved to the recording chamber containing the patch pipette solution (IPS), which consisted of (in mM) 140 KCl, 1 $MgCl_2$, 5 HEPES, 1 $CaCl_2$, 5 EGTA, and pH adjusted to 8.0 with KOH. The recording compartment was connected via a 3 M KCl/agar bridge to a ground compartment. After excision, solutions were added to the recording compartment through an inflow tube. Bath volume was ~0.3–0.4 ml and total volume exchange occurred within 5–10 s. Hemichannel currents were recorded in cell-attached and excised-patch configurations using an Axopatch one-dimensional amplifier (Axon Instruments Inc., Union City, CA.). Currents were filtered at 1 kHz and data were acquired at 5 kHz. All recordings, both at macroscopic and single hemichannel level were acquired using an AT-MIO-16X D/A board from National Instruments (Austin, TX) and acquisition software written by E. B. Trexler, Mount Sinai School of Medicine, NY.

RESULTS

Cysteine Substitution at Phe^{43} of Cx50 Leads to Impairment of Hemichannel Function—Cx50 and Cx46, the principal lens connexins closely related in sequence, produce large membrane currents when expressed in oocytes that decline for negative and positive voltages as previously described (13–16). The decline in conductance with hyperpolarization is ascribed to loop gating and is selectively modulated by extracellular divalent cations, which suppress the current and shift activation positive along the voltage axis; gating at positive voltages (V_j gating) does not appear to be regulated by extracellular divalent cations (8). In addition, loop gating in Cx50 exhibits a robust potentiation in response to increases in extracellular K^+, a property that acts through modulation of Ca^{2+} sensitivity (16). An example of the behavior of WT Cx50 hemichannels in response to changes in extracellular Ca^{2+} and K^+ is shown in Fig. 1*A*. An oocyte expressing WT Cx50 voltage clamped to a holding potential of −40 mV typically develops a large inward current upon lowering extracellular Ca^{2+} from 1.8 to 0.2 mM. Replacement of extracellular Na^+ with K^+ while maintaining Ca^{2+} at 0.2 mM further potentiates the current.

To identify residues involved in gating at hyperpolarized membrane potentials, we engineered cysteines at a number of positions at the TM1/E1 border in Cx50. We initially focused on residue 43 because it was shown to be an important determinant of the difference in gating exhibited by Cx46 and Cx50 hemichannels (9). Upon substituting a cysteine residue for the phenylalanine at position 43 (F43C) in Cx50, hemichannel function was significantly impaired. No appreciable increase in membrane current was evident upon lowering extracellular Ca^{2+} to 0.2 mM and there was only a modest increase when bath Na^+ was replaced by K^+ (Fig. 1*B*). Because of the possibility that impaired function resulted from disulfide bond formation, we applied the reducing agent, DTT. In the presence of KCl solutions containing 0.2 mM Ca^{2+}, application of DTT (100 μM) caused a large inward current to develop, similar to that observed for oocytes expressing WT Cx50. In the illustrated example, baseline current increased from 0.5 to 6.4 μA, corresponding to a 13-fold increase. The effect of DTT was rapid and reversible upon washout, although recovery was generally slow, taking several minutes for the current to return to the baseline level prior to DTT application. A family of voltage steps applied to an oocyte expressing F43C with and without DTT shows little or no detectable current in the absence of DTT and robust currents resembling those of WT Cx50 in the presence of DTT (Fig. 1*C*). The increase in current caused by 100 μM DTT was always observed in F43C-expressing oocytes. In contrast, no potentiation by DTT was observed in oocytes expressing WT Cx50 (see below) or in uninjected oocytes.

DTT, in addition to being a reducing agent, can also chelate metal ions with high affinity, *e.g.* K_D for binding to $Zn^{2+} \sim 10^{-10.3}$ M (17). Thus, it is possible that impaired function of F43C hemichannels is due to metal binding and restoration of function by DTT is the result of chelation rather than reduction of disulfide bonds. To distinguish between these possibilities, we applied TPEN, a highly specific transition metal chelating agent (*e.g.* K_D for binding to $Zn^{2+} \sim 10^{-15.6}$ M) that has no reducing capacity, as well as low affinity for Ca^{2+}, $K_D \sim 10^{-4.4}$ M, and Mg^{2+}, $K_D \sim 2 \times 10^{-1.7}$ M (18). As shown in Fig. 2*A*, exposure of an oocyte expressing F43C to a low concentration of TPEN (10 μM) produced a robust increase in current. A higher concentration of TPEN (20 μM) produced no additional increase suggesting a maximal effect was achieved at 10 μM (data not shown). As with DTT, the effect of TPEN was rapid in onset and slower to reverse. The potentiation caused by TPEN was essentially the same magnitude as that caused by DTT and effects of TPEN and DTT when applied together were not additive, suggesting that both agents act by the same mechanism, *i.e.* chelation of metal ions present in our experimental solutions and/or in oocytes. Cysteine substitution at position 43 in Cx46 (E43C) also led to potentiation by DTT and TPEN. However, E43C hemichannel currents in the absence of chelators were larger and correspondingly the magnitude of the potentiation caused by DTT or TPEN was smaller, ~3-fold. Mean values for potentiation by TPEN and DTT in WT and cysteine-substituted Cx46 and Cx50 are summarized in Fig. 2*B*. Neither DTT nor TPEN at the same concentrations affected wild-type Cx50

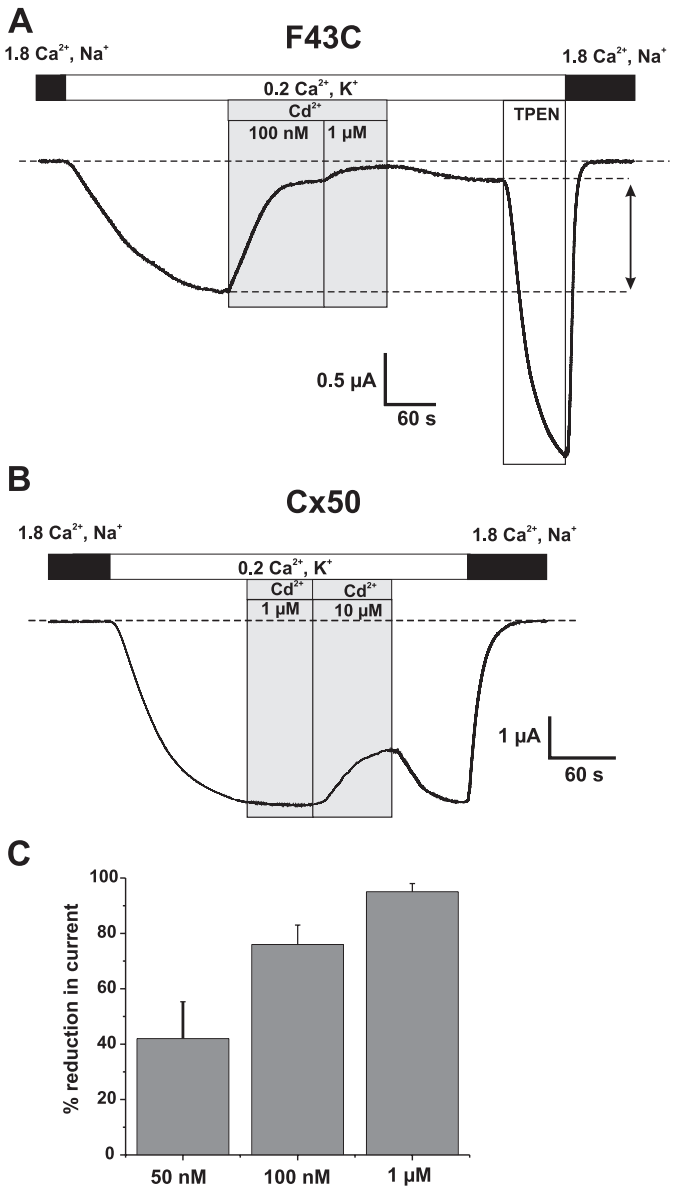

FIGURE 3. **F43C hemichannels exhibit high-affinity binding to metal ions.** *A*, shown are membrane currents in an oocyte voltage clamped at −40 mV. Application of Cd^{2+} caused a strong reduction in the inward current in a concentration dependent manner with 100 nM and 1 μM reducing currents by ~80 and ~95%, respectively. Perfusion of oocytes with Cd^{2+}-free solution caused only a modest recovery of current (~30% of control), indicating that Cd^{2+}-bound hemichannels are locked closed. Recovery of channel activity after Cd^{2+} block required TPEN. The increase in inward current caused by TPEN was substantially higher in magnitude compared with the current before Cd^{2+} application, indicating that a large fraction of hemichannels were locked closed. *B*, the same concentrations of Cd^{2+} have no effect on Cx50 WT hemichannels. Inhibition of wild-type hemichannels occurs only at substantially higher concentrations (10 μM) and was fully reversible upon washout. *C*, *bar graph* summarizing the effect of 50 nM ($n = 9$), 100 nM ($n = 8$) and 1 μM ($n = 16$) Cd^{2+} on F43C hemichannels. *Bars* represent the mean ± S.E. of block. The concentration dependence indicates half-maximal reduction in current occurring between 50 and 100 nM for Cd^{2+}.

or Cx46 hemichannels. Addition of EGTA to the bath also potentiated F43C and E43C currents (data not shown), but the effect was compounded by strong chelation of Ca^{2+} as well. These results indicate that an introduced cysteine at position 43 participates in the formation of high affinity metal bridges, leading to impaired function or "lock-up" of hemichannels in a

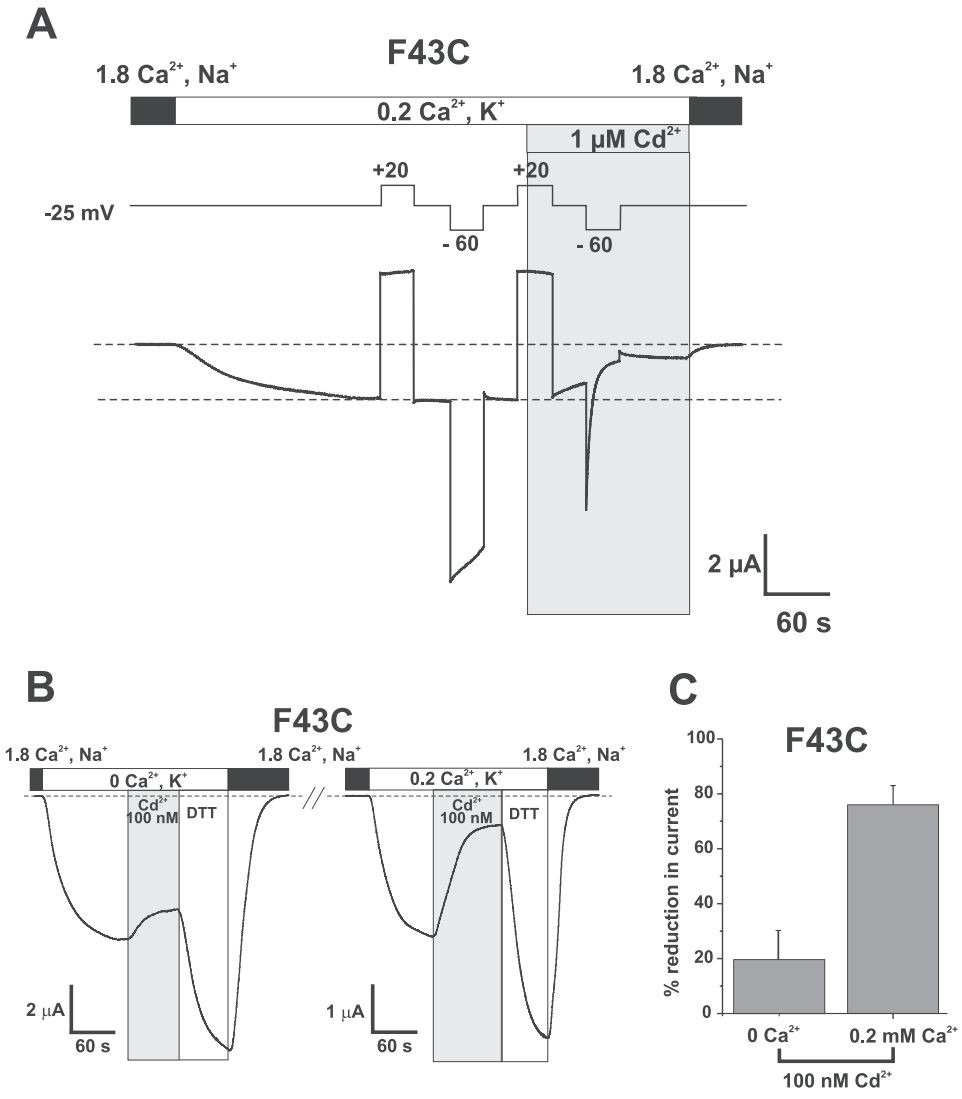

FIGURE 4. **Cd^{2+} block of F43C hemichannels is promoted during closure by hyperpolarization and extracellular Ca^{2+}.** *A*, an oocyte expressing F43C was voltage clamped at −25 mV and extracellular Ca^{2+} was lowered to 0.2 mM in a KCl solution. A pair of 30-s voltage steps were applied, one depolarizing to +20 mV to place F43C channels in the open state and one hyperpolarizing to −60 mV to promote closure of the loop gate. Application of 1 μM Cd^{2+} at +20 mV (*shaded area*) produced little or no block of the outward current. However, subsequent hyperpolarization to −60 mV in the continued presence of Cd^{2+} caused a rapid reduction in the current, indicating that the introduced cysteines move during loop gating and form metal bridges. *B*, shown are membrane currents in an oocyte voltage clamped at −30 mV. Perfusing a KCl solution containing no added Ca^{2+} (0 Ca^{2+}, K^+) produced a substantial inward current. Application of 100 nM Cd^{2+} produced a modest reduction in current of ~20%. Brief application of DTT increased current beyond that in 0 mM Ca^{2+} alone indicating there was some modest lock-up. Changing a KCl solution containing 0.2 mM Ca^{2+} (0.2 Ca^{2+}, K^+) decreased the current (note change in scale) and addition of the same 100 nM concentration of Cd^{2+} now produced a substantial reduction in current of ~75%. Brief application of DTT similarly increased current beyond levels in 0.2 mM Ca^{2+} alone. *C*, *bar graph* summarizing the effect of 100 nM Cd^{2+} applied at −30 mV in 0 mM Ca^{2+} ($n = 5$) and 0.2 mM Ca^{2+} ($n = 8$). *Bars* represent the mean ± S.E. of block.

non-conducting or a low-conducting state. Lock-up was more pronounced for Cx50 than Cx46 hemichannels, likely reflecting subtle conformational and/or sequence differences. Such differences are supported by biophysical data showing different gating characteristics upon hyperpolarization (9, 15).

F43C Hemichannels Exhibit High Sensitivity to Cd^{2+}—Release of F43C hemichannels from lock-up by TPEN indicates that the oocytes and/or the bath solutions contain some contaminating transition metal ions. Use of solutions containing low contaminating metals did not alleviate lock-up (data not shown). We also observed that F43C currents increased several days after mRNA injection and were accompanied by concomitant reductions in the magnitude of the potentiation produced by DTT or TPEN (data not shown). Taken together, these data suggests that endogenous metal ions in the oocyte cytoplasm, such as Zn^{2+}, may be largely responsible for lock-up and can deplete over time.

To confirm that cysteine substitution at Phe^{43} introduces high-affinity metal binding, we examined sensitivity to Cd^{2+} bath-applied to oocytes several days after injecting mRNA, when F43C-expressing oocytes exhibit modest currents in low Ca^{2+} (0.2 mM) KCl solutions without exposure to DTT or TPEN. Application of as little as 50 nM Cd^{2+} caused substantial reductions in current. In the example shown (Fig. 3), an oocyte voltage clamped to −40 mV was exposed to a 0.2 mM Ca^{2+}-containing KCl solution, which produced an inward current of ~2.5 μA. Application of 100 nM and 1 μM Cd^{2+} reduced the current by ~80 and ~95%, respectively (Fig. 3*A*). Upon washout with a Cd^{2+}-free solution, the current did not recover appreciably indicating that the hemichannels essentially remained locked-up; a small degree of recovery (up to 20–30%) was typical. Application of TPEN relieved the lock-up induced by Cd^{2+} and further increased the current beyond the control level indicative that there was lock-up from endogenous metals as well as exogenously added Cd^{2+}. In contrast, WT Cx50 hemichannels showed no sensitivity to Cd^{2+} at these low concentrations. Inhibition of WT Cx50 hemichannel currents by Cd^{2+} could be seen at ~100-fold higher concentrations and exhibited different characteristics, in particular showing rapid and full reversibility upon washout (Fig. 3*B*), consistent with the typical sensitivity exhibited by connexin hemichannels to divalent cations (16, 19). Mean reductions in current for three different concentrations of Cd^{2+} on F43C channels are summarized in Fig. 3*C* and show that there is high affinity binding with an half-maximal reduction in current occurring in the range of 50–100 nM. Similar sensitivity was found for Zn^{2+} (data not shown). These results indicate that introduction of a cysteine at position 43 produces a novel high-affinity metal binding site.

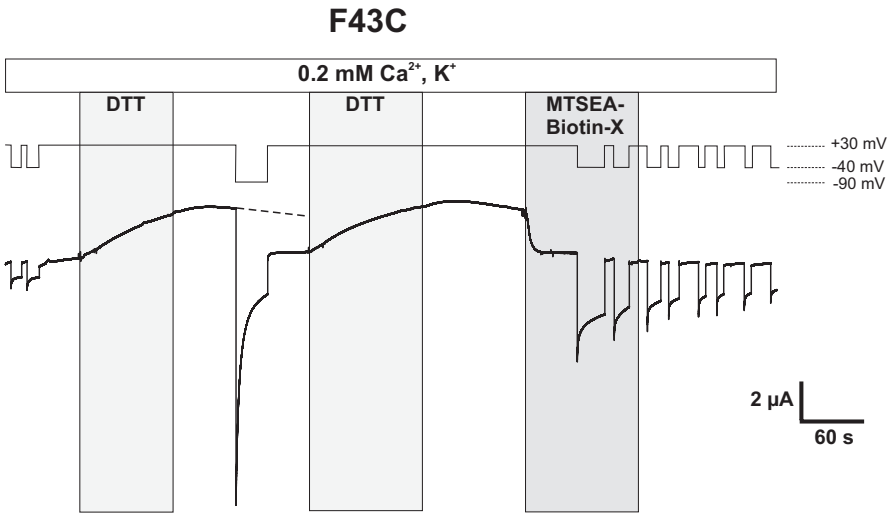

FIGURE 5. **Phe^{43} forms part of aqueous pore in Cx50.** Shown is a macroscopic recording from a F43C-expressing oocyte voltage clamped at −40 mV in 0.2 mM Ca^{2+}-containing KCl solutions. Voltage steps to +30 mV did not cause activation of membrane currents, consistent with lock-up. Application of DTT (100 μM) while the membrane potential was held at +30 mV elicited a large increase in the outward current. Washout of DTT did not cause a substantial decrease in current magnitude at +30 mV; however, hyperpolarization to −90 mV produced a rapid decrease in the current that remained low in magnitude even after a second depolarizing pulse to +30 mV, consistent with the state-dependent lock-up. Application of MTSEA-biotin to open F43C channels after the second application and washout of DTT produced a strong and rapid decrease in current, indicating accessibility of Phe^{43} in the open state. The effect of MTS reagent remained after washout as expected for covalent binding of the reagent to F43C.

Lock-up of F43C Hemichannels by Cd^{2+} Is Promoted by Conditions That Promote Closure—Both hyperpolarization and extracellular divalent cations, alone or in combination, promote hemichannel closure (8). Thus, we examined the relationship between lock-up by Cd^{2+} and gating induced by hyperpolarization (Fig. 4*A*) and Ca^{2+} (Fig. 4, *B* and *C*). An oocyte expressing F43C was voltage clamped to −25 mV and a moderate depolarizing step to +20 mV was applied to place the hemichannels in an open configuration (Fig. 4*A*). Subsequent application of a hyperpolarizing step to −60 mV produced moderate closure by loop-gating that recovered upon repolarizing back to −25 mV. Repeating the same protocol and applying Cd^{2+} (1 μM) at +20 mV caused only a small reduction in current. However, upon hyperpolarization to −25 mV in the continued presence of Cd^{2+}, the current declined more notably and subsequent hyperpolarization to −60 mV produced a robust and rapid decline in current that did not recover even after polarizing back to −25 mV.

Fig. 4, *B* and *C*, show a comparison of the effects of Cd^{2+} on F43C hemichannels when varying extracellular Ca^{2+}. In an oocyte held at −30 mV, a voltage where F43C hemichannels primarily remain open in the absence of added Ca^{2+}, addition of 100 nM Cd^{2+} produced only a small reduction (~20%) in current (Fig. 4*B*). Addition of 0.2 mM Ca^{2+} caused a decrease in the magnitude of the current as a result of gating (note change in scale) and the same 100 nM concentration of Cd^{2+} now produced a substantial reduction (~75%) in current. *Bar graphs* summarizing mean reductions in current by 100 nM Cd^{2+} at both Ca^{2+} concentrations illustrate the dramatic difference in sensitivity to Cd^{2+}. Thus, the effect of Cd^{2+} is more pronounced at more hyperpolarized potentials (Fig. 4*A*) and/or at higher Ca^{2+} concentrations (Fig. 4, *B* and *C*), indicating that the engineered Cys residues move into close proximity to each other or to other residues during gating thereby allowing coordination of Cd^{2+}.

Phe^{43} Resides in the Pore in the Open State of Cx50 Hemichannels—The results described thus far are consistent with the residue at position 43 undergoing movement during loop gating in Cx50 as well as Cx46 hemichannels. Previous studies in Cx46 hemichannels using the substituted-cysteine accessibility method (SCAM) showed that Glu^{43} resides in the pore in the open state (10). To determine whether Phe^{43} in Cx50 is similarly pore-lining, we used SCAM to assess accessibility of F43C to MTS reagents. Fig. 5*A* shows a recording from an oocyte expressing F43C held at −40 mV. Repeated voltage steps to +30 mV showed little activation consistent with lock-up. Application of DTT, while holding the potential at +30 mV, produced a large outward current that did not decrease appreciably after wash-out of DTT. However, hyperpolarization to −90 mV caused a rapid reduction in current that remained significantly reduced upon depolarizing the membrane back to +30 mV, consistent with a state-dependent lock-up. After a second treatment and washout of DTT at +30 mV, application of the thiol reagent MTSEA-biotin-X produced an immediate and large reduction in current, ~75%, that did not reverse upon washout indicative of covalent modification. This effect was not observed in WT Cx50 hemichannels (data not shown).

To ensure that the decrease in macroscopic current produced by application of an MTS reagent was due to modification of a pore-lining residue, we applied SCAM at the single hemichannel level in excised patches (10) where we could monitor changes in open hemichannel conductance and assess accessibility from either side of the membrane. Using MTSEA-biotin as the thiol reagent, modification of a single F43C hemichannel is illustrated in Fig. 6. Bath application of MTSEA-biotin (~100–200 μM) to a single F43C hemichannel in an inside-out patch produced a strong decrease in the unitary current amplitude within seconds of application (Fig. 6). In this patch configuration, where the cytoplasmic aspect of the hemichannel is exposed to the bath, MTSEA-biotin would have to traverse much of the length of the hemichannel to reach F43C at the extracellular membrane border. Reductions in unitary current occurred in a stepwise fashion, showing 5 to 6 discrete steps consistent with modifications occurring on individual connexin subunits (*arrows* in Fig. 6). The final conductance remained stable after washout; comparison of the I-V curves of the same hemichannel before and 3 min after application and washout of MTSEA-biotin illustrates the robust and permanent change in unitary current over a large voltage range (Fig. 6*B*). The same magnitude and step-

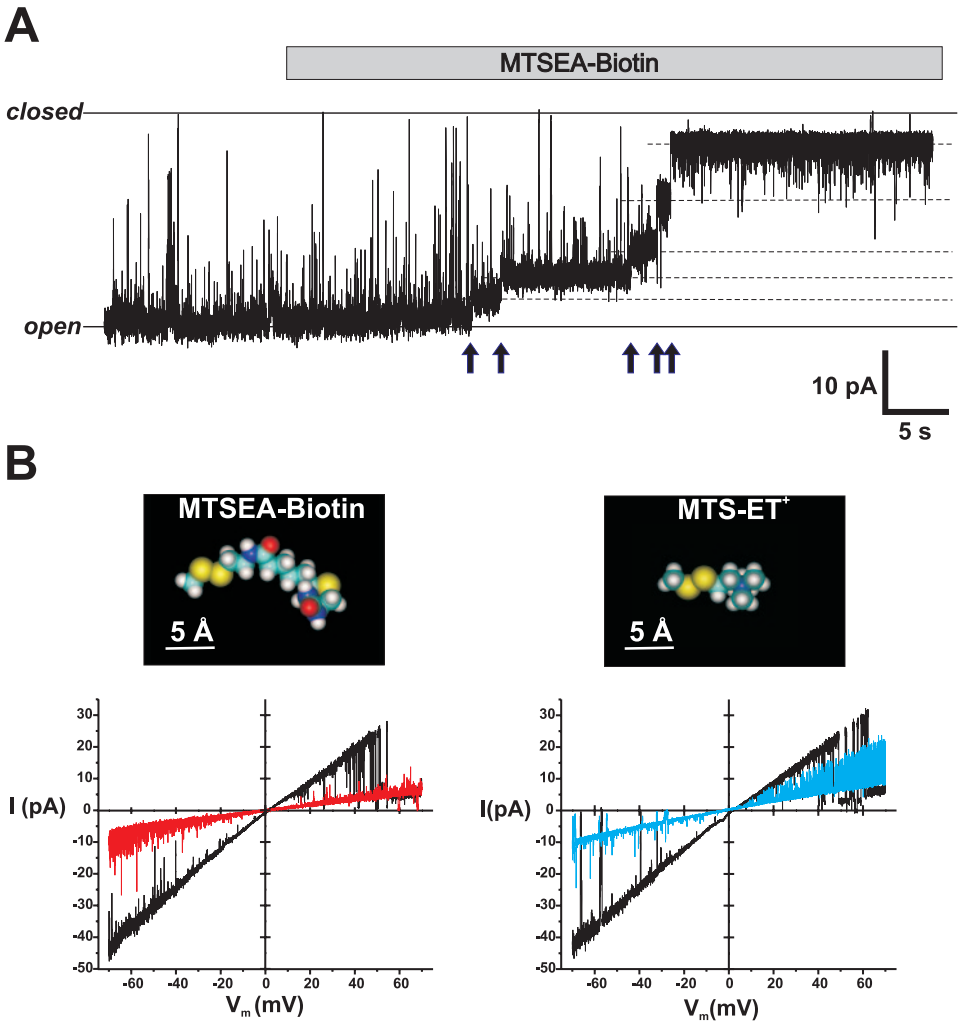

FIGURE 6. **Single channel SCAM indicates that Phe[43] is a pore-lining residue.** *A*, example of MTSEA-biotin modification of a single F43C hemichannel recorded in the inside-out patch configuration. The membrane potential was held at −50 mV. Application of MTSEA-biotin (100 μM) caused a stepwise reduction in the single hemichannel current (*arrows*). At least five distinct changes in current can be observed indicating modification of individual cysteines. *B*, comparison of single open hemichannel I-V curves of the same F43C hemichannel obtained before (*solid trace*) and 3 min after application and subsequent washout of MTSEA-biotin (*left panel*, *red trace*) or MTS-ET$^+$ (*right panel*, *blue trace*) showing reduction in channel conductance by MTS reagents.

wise reduction in current occurred on F43C hemichannels in outside-out patches (data not shown) indicating F43C is accessible from either side of the membrane as expected for a residue located in the aqueous pore. A robust reduction in conductance also was obtained with the smaller positively charged thiol reagent MTS-ET$^+$ (Fig. 6*C*), but differed in magnitude and had different characteristics, namely the decrease in unitary conductance with MTS-ET$^+$ was smaller and the resulting open hemichannel current was less noisy, which presumably reflects the smaller size and motions of the introduced side chains. Slope conductance was reduced from 527 to 155 pS and 77 pS by MTS-ET$^+$ and MTSEA-biotin, respectively.

Other Pore-lining Residues and Gating—Previously in Cx46 hemichannels, we showed that in addition to Glu[43], Gly[46] and Asp[51] within the E1 domain face the lumen of the hemichannel pore in the open state (10). Thus, we engineered cysteine substitutions at the corresponding Gly[46] and Asp[51] residues in Cx50, as well as some nearby residues, Ala[40], Ala[41], and Glu[42]. The results are summarized in Fig. 7. As in Cx46, G46C and D51C, but not A40C and A41C, were found to reside in the pore in the open state in Cx50 (Fig. 7*A*). These assignments were based on SCAM studies in single Cx50 hemichannels in which MTSEA-biotin applied from either side membrane irreversibly reduced unitary conductance. The E42C substitution in Cx50, as previously shown in Cx46, did not produce functional hemichannels. Like F43C, G46C hemichannel currents were robustly potentiated by both TPEN and DTT and exhibited strong sensitivity to 1 μM Cd^{2+} (Fig. 7*B*). D51C exhibited substantially less potentiation by TPEN and DTT and correspondingly less sensitivity to Cd^{2+} (Fig. 7*B*). Also, the effects of Cd^{2+} at D51C were readily reversible, suggesting that coordination was not optimal. A40C and A41C, which were not pore-lining, showed no evidence of high-affinity metal binding as indicated by the absence of potentiation by DTT or TPEN and lock-up by Cd^{2+}. These results show a correlation between residence in the pore and metal binding indicating that movements associated with loop gating position pore-lining residues in the TM1/E1 region, specifically F43C and G46C, where they have the ability to form high-affinity metal bridges.

DISCUSSION

In this study, we demonstrate that residues at the putative TM1/E1 border of Cx50 are an integral part of the structural rearrangement that occurs during loop gating. Supportive evidence that the extracellular loops play a central role in loop gating comes from biophysical data accrued from WT and modified hemichannels. First, loop gating transitions are characterized by a series of transient subconductance states en route to full opening/closure (5, 15) that resemble docking transitions associated with opening of newly formed gap junction channels (20), a process for which the extracellular loops undoubtedly play a central role. Second, loop gating is also strongly influenced by extracellular, but not intracellular Ca^{2+} (8). Finally, studies in Cx46 hemichannels on the state-dependent accessibility of thiol-specific reagents suggest the existence of a gate located in the extracellular half of TM1 or in E1 (21).

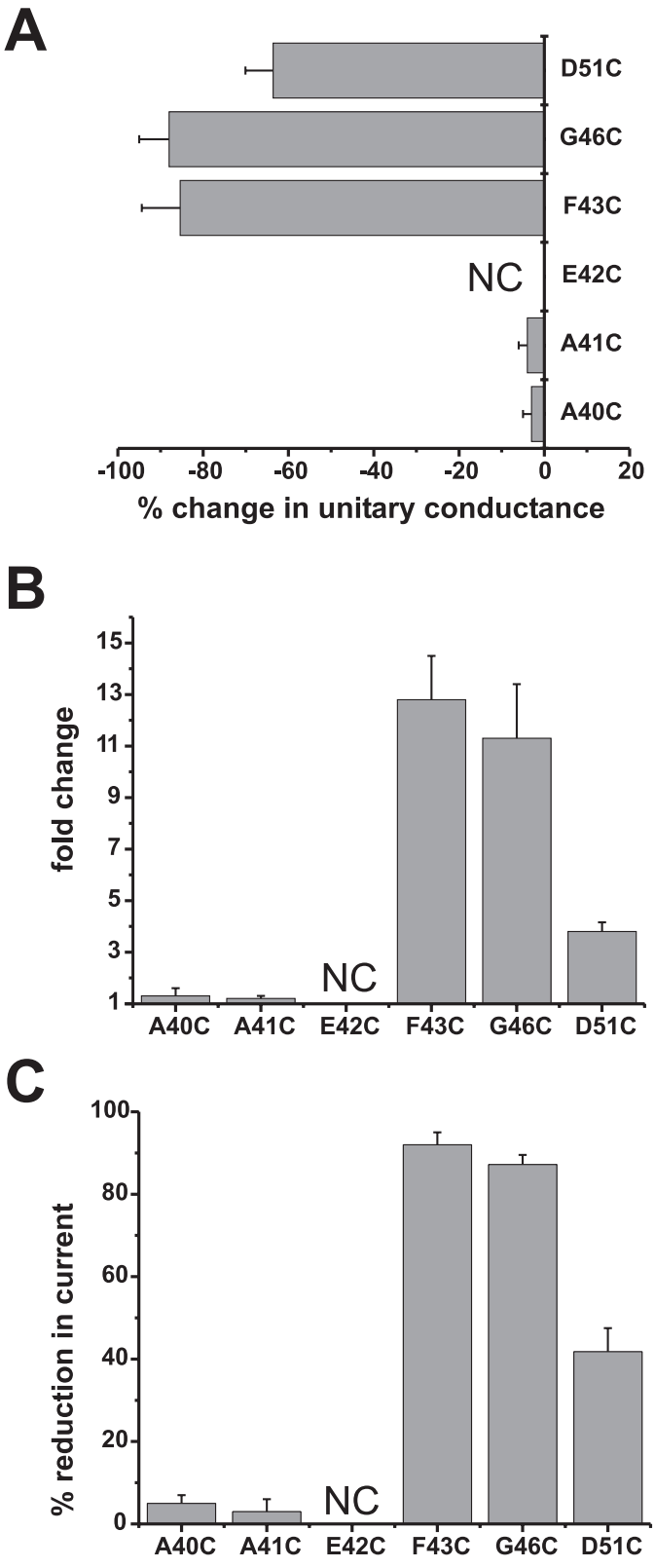

FIGURE 7. **Correspondence between residence in the pore and metal binding.** *A*, SCAM using MTSEA-biotin shows three residues in E1 accessible to modification in single open hemichannels. Shown is a plot of the percentage change in unitary conductance for each residue after application of 100 μM MTSEA-biotin. The change in unitary conductance represents the mean percentage change in the slope conductance (measured at $V_m = 0$ from fitted open channel I-V relations) caused by MTS-biotin relative to unmodified cysteine-substituted channels for each mutant. Reductions in conductance were observed at three positions, F43C ($n = 7$), G46C ($n = 7$), and D51C ($n = 6$), but not at A40C ($n = 5$) or A41C ($n = 5$). *B* and *C*, potentiation by 100 μM DTT (*B*) and block by 1 μM Cd^{2+} (*C*) was robust for pore-lining residues F43C and G46C. D51C also was affected by DTT and Cd^{2+}, but the magnitudes of changes were weaker in comparison. A40C and A41C hemichannels were not affected by DTT or Cd^{2+}. Oocytes were voltage clamped to −40 mV. *Bars* represent the mean ± S.E. of the potentiation produced by DTT or block produced by Cd^{2+} (*n* ranged from 7 to 18).

Cysteine substitutions at pore-lining residues Phe^{43}, Gly^{46}, and to a lesser extent Asp^{51}, but not at nearby non-pore-lining residues, led to high-affinity metal binding, manifested as lock-up in a closed or poorly functional state promoted by membrane hyperpolarization and/or extracellular Ca^{2+}, both conditions that alone or in combination favor hemichannel closure. The binding affinity for Cd^{2+} both in F43C and G46C hemichannels is high, as evidenced by the substantial effects observed with as little as 100 nM Cd^{2+}, and lock-up induced by hyperpolarization did not reverse readily even with depolarization, requiring application of chelators such as DTT or TPEN. These data are indicative of metal ion coordination involving two or more residues. Bath application of 1 μM Cd^{2+} to D51C hemichannels also produced a reduction in current, but it was smaller and essentially reversible within a few minutes of washout, *i.e.* it exhibited little in the way of lock-up. The correlation between metal ion binding and residence in the pore, albeit weaker at D51C, suggests that metal ions access the substituted cysteine side chains through the aqueous pore. Given that high-affinity metal binding is not evident in the open state and that the connexin pore is large (22–25), hemichannel closing likely involves considerable movement such that the sulfhydryl groups of F43C or G46C, which are not in close proximity in the open state, become close enough to each other or to other residues to form at least bidentate metal binding sites. Although metal ions could conceivably interact with individual cysteines and cause a reduction in unitary current at any voltage, affinity for such monodentate binding would be low, and thus masked by the robust gating effects exhibited by divalent metal ions in connexin hemichannels.

In the absence of a high-resolution structure for connexins, it is difficult to speculate about the positions and movements of the Phe^{43}, Gly^{46}, and Asp^{51} residues on an atomic scale. If coordination of metal ions is occurring among the F43C or G46C residues during closure, it would imply that the pore is undergoing a substantial constriction in this region from one that can accommodate multiple MTSEA-biotin moieties in the open state to one that brings the cysteine side chains to within ~3–4 Å during closure. Although not quantified, MTSEA-biotin or -biotin-X reactions at F43C and G46C in Cx50 did appear to impede closure (data not shown) consistent with imposition of a steric constraint on gating. The apparent lack of coordination at D51C may indicate less movement in this region or that the movements during gating do not bring D51C side chains into an orientation favorable for metal coordination or into close enough proximity, perhaps suggestive of a wider pore in this region. Electron crystallographic images of two connexins, Cx43 and Cx26, have been obtained (23, 26) and the gross overall topology of these gap junction channels show pronounced narrowing of the pore at the outer membrane borders where Phe^{43} and Gly^{46} are putatively located. Although both struc-

tures were obtained under conditions that are known to promote closure, the state of the channels is unknown and resolution remains insufficient to see details of secondary structure. Given that there is the potential for close proximity of F43C and G46C residues during gating, and that there may be considerable flexibility in this region, it is reasonable to expect the possibility of disulfide bond formation. However, we saw no evidence of this electrophysiologically as TPEN and DTT gave the same results and there was no additional effect of DTT after TPEN application. It is possible that the distance and orientation of the cysteine residues is unfavorable for disulfide bond formation. Alternatively, metal coordination may involve cysteine and non-cysteine residues (*e.g.* glutamic acid etc.).

Although structural models providing details of the atomic scale movements that occur in connexins during gating are lacking, models obtained from high-resolution structures of other large-pore ion channels provide some useful comparisons. One such class of channels is the mechanosensitive ion channels belonging to the MscL family, which share some interesting biophysical characteristics with connexins. For one, opening of an MscL channel proceeds through a series of transient substates and is believed to represent a disruption of the closed state in sequential steps (27). This type of multistep gating transition is very similar to that which occurs in connexins during loop gating, as originally described in Cx46 by Trexler *et al.* (5) and subsequently in other connexin hemichannels (5, 15, 28, 29). Although loop gating is inherently voltage dependent (8), whereas opening of MscL channels is initiated by membrane tension, some connexin hemichannels, such as Cx46, have been shown to exhibit mechanosensitivity (30). In MscL channels, mutations that have a strong effect on gating were shown to map to residues along one side of the TM1 helix, the side that faces the aqueous pore (31). In Cx50 hemichannels, we see a correlation between pore-lining residues at the TM1/E1 border and loop gating. Such a correlation between gating and residence in the pore is explained, perhaps, by a mechanism that involves the breaking up of a closed gate formed by interacting hydrophobic, pore-lining residues. In Cx50, only one of the three identified pore-lining residues, Phe^{43}, is hydrophobic, but hydrophobicity of this position is not conserved among connexins. In Cx46 hemichannels, identification of pore-lining residues extended further into TM1, and included two additional residues, Ala^{39} and Leu^{35} (10); the latter residue putatively lies midway within the TM1 span. It is in this region of TM1, as well as the segment proceeding toward the cytoplasmic NH_2 terminus, where a number of hydrophobic residues are conserved. Interestingly, cysteine mutations in this hydrophobic region were shown to severely affect gating and several mutants did not function or functioned poorly (32), perhaps indicative of disrupted hydrophobic interactions that play an important role in gating. In this view, TM1 can be analogous to pore-lining domains of other large-pore ion channels, such as MscL and AChRs, which use pore-lining hydrophobic residues to form an effective barrier to ionic flux (33).

Recently, an electron crystallographic structure of a Cx26 gap junction channel containing a mutation in TM1 was obtained at 10-Å resolution in the membrane plane and showed the channel pore blocked by a "central gate" or "plug" representing a density formed by six interacting cytoplasmic domains (26). This structure was postulated to be an occluding gate made by interacting NH_2 termini whose movement into and out of the pore represents gating. At present, however, it is unknown whether this structure is linked to the movements at the TM1/E1 border or whether it even represents a physiological state of connexins. It must be noted that gating to a stable, residual substate, the so-called V_j gating, is a gating mechanism distinct from loop gating, which in Cx50 and Cx46 occurs at positive potentials. V_j gating has been shown to principally involve movement of the NH_2 terminus (34–37), and likely represents a different conformational state that leaves the channel partially occluded. Which gating mechanism, if any, the central-plug structure represents has not been resolved.

Proposed functions of hemichannels include release of signaling molecules such as glutamate and ATP (38–41). Pathogenic functions of hemichannels, particularly formed of the structurally related pannexins, include contributions to neuronal excitotoxicity after ischemia (42) suggesting hemichannels can participate in cell death, most likely by mediating loss of cellular metabolites or excessive entry of extracellular ions. Opening of unapposed hemichannels appears to be effectively controlled by loop gating via its robust sensitivity to voltage and extracellular divalent cations. Other factors have also been shown to influence hemichannel opening, such as metabolic inhibition and intracellular Ca^{2+} (43–45). Whether all these mechanisms act through loop gating remains unknown, but it has been suggested that modulators of connexin channels and hemichannels, such as pH, quinine, and long-chain alkanols, may converge on loop gating making it a potential common mechanism of closure acted on by diverse stimuli (1, 2, 46).

REFERENCES

1. Harris, A. L. (2001) *Q. Rev. Biophys.* **34,** 325–472
2. Bukauskas, F. F., and Verselis, V. K. (2004) *Biochim. Biophys. Acta* **1662,** 42–60
3. Bukauskas, F. F., Elfgang, C., Willecke, K., and Weingart, R. (1995) *Biophys. J.* **68,** 2289–2298
4. Trexler, E. B., Bukauskas, F. F., Kronengold, J., Bargiello, T. A., and Verselis, V. K. (2000) *Biophys. J.* **79,** 3036–3051
5. Trexler, E. B., Bennett, M. V., Bargiello, T. A., and Verselis, V. K. (1996) *Proc. Natl. Acad. Sci. U. S. A.* **93,** 5836–5841
6. Ebihara, L., Liu, X., and Pal, J. D. (2003) *Biophys. J.* **84,** 277–286
7. Puljung, M. C., Berthoud, V. M., Beyer, E. C., and Hanck, D. A. (2004) *J. Gen. Physiol.* **124,** 587–603
8. Verselis, V. K., and Srinivas, M. (2008) *J. Gen. Physiol.* **132,** 315–327
9. Tong, J. J., and Ebihara, L. (2006) *Biophys. J.* **91,** 2142–2154
10. Kronengold, J., Trexler, E. B., Bukauskas, F. F., Bargiello, T. A., and Verselis, V. K. (2003) *J. Gen. Physiol.* **122,** 389–405
11. Verselis, V. K. (2009) in *Connexins: A Guide* (Harris, A. L., and Locke, D., ed) pp. 77–102, Humana Press, New York, NY
12. Karlin, A., and Akabas, M. H. (1998) *Methods Enzymol.* **293,** 123–145
13. Zampighi, G. A., Loo, D. D., Kreman, M., Eskandari, S., and Wright, E. M. (1999) *J. Gen. Physiol.* **113,** 507–524
14. Beahm, D. L., and Hall, J. E. (2002) *Biophys. J.* **82,** 2016–2031
15. Srinivas, M., Kronengold, J., Bukauskas, F. F., Bargiello, T. A., and Verselis, V. K. (2005) *Biophys. J.* **88,** 1725–1739
16. Srinivas, M., Calderon, D. P., Kronengold, J., and Verselis, V. K. (2006) *J. Gen. Physiol.* **127,** 67–75
17. Krzel, A., Lesniak, W., Jezowska-Bojczuk, M., Mlynarz, P., Brasun, J., Kozlowski, H., and Bal, W. (2001) *J. Inorg. Biochem.* **84,** 77–88
18. Arslan, P., Di Virgilio, F., Beltrame, M., Tsien, R. Y., and Pozzan, T. (1985)

J. Biol. Chem. **260,** 2719–2727
19. Ebihara, L., and Steiner, E. (1993) *J. Gen. Physiol.* **102,** 59–74
20. Bukauskas, F. F. (2001) *Methods Mol. Biol.* **154,** 379–393
21. Pfahnl, A., and Dahl, G. (1998) *Biophys. J.* **75,** 2323–2331
22. Wang, H. Z., and Veenstra, R. D. (1997) *J. Gen. Physiol.* **109,** 491–507
23. Unger, V. M., Kumar, N. M., Gilula, N. B., and Yeager, M. (1999) *Science* **283,** 1176–1180
24. Verselis, V. K., and Veenstra, R. D. (2000) in *Gap Junctions* (Hertzberg, E. L., ed) Vol. 30, pp. 129–192, JAI Press, Stamford, CA
25. Valiunas, V., Beyer, E. C., and Brink, P. R. (2002) *Circ. Res.* **91,** 104–111
26. Oshima, A., Tani, K., Hiroaki, Y., Fujiyoshi, Y., and Sosinsky, G. E. (2007) *Proc. Natl. Acad. Sci. U. S. A.*
27. Sukharev, S., Betanzos, M., Chiang, C. S., and Guy, H. R. (2001) *Nature* **409,** 720–724
28. Oh, S., Abrams, C. K., Verselis, V. K., and Bargiello, T. A. (2000) *J. Gen. Physiol.* **116,** 13–31
29. Valiunas, V., and Weingart, R. (2000) *Pflugers Arch.* **440,** 366–379
30. Bao, L., Sachs, F., and Dahl, G. (2004) *Am. J. Physiol.* **287,** C1389–C1395
31. Chang, G., Spencer, R. H., Lee, A. T., Barclay, M. T., and Rees, D. C. (1998) *Science* **282,** 2220–2226
32. Kronengold, J., Trexler, E. B., Bukauskas, F. F., Bargiello, T. A., and Verselis, V. K. (2003) *Cell Commun. Adhes.* **10,** 193–199
33. Doyle, D. A. (2004) *Trends Neurosci.* **27,** 298–302
34. Verselis, V. K., Ginter, C. S., and Bargiello, T. A. (1994) *Nature* **368,** 348–351
35. Ri, Y., Ballesteros, J. A., Abrams, C. K., Oh, S., Verselis, V. K., Weinstein, H., and Bargiello, T. A. (1999) *Biophys. J.* **76,** 2887–2898
36. Purnick, P. E., Benjamin, D. C., Verselis, V. K., Bargiello, T. A., and Dowd, T. L. (2000) *Arch. Biochem. Biophys.* **381,** 181–190
37. Purnick, P. E., Oh, S., Abrams, C. K., Verselis, V. K., and Bargiello, T. A. (2000) *Biophys. J.* **79,** 2403–2415
38. Stout, C. E., Costantin, J. L., Naus, C. C., and Charles, A. C. (2002) *J. Biol. Chem.* **277,** 10482–10488
39. Zhao, H. B., Yu, N., and Fleming, C. R. (2005) *Proc. Natl. Acad. Sci. U. S. A.* **102,** 18724–18729
40. Genetos, D. C., Kephart, C. J., Zhang, Y., Yellowley, C. E., and Donahue, H. J. (2007) *J. Cell. Physiol.* **212,** 207–214
41. Schock, S. C., Leblanc, D., Hakim, A. M., and Thompson, C. S. (2008) *Biochem. Biophys. Res. Commun.* **368,** 138–144
42. Thompson, R. J., Zhou, N., and MacVicar, B. A. (2006) *Science* **312,** 924–927
43. John, S. A., Kondo, R., Wang, S. Y., Goldhaber, J. I., and Weiss, J. N. (1999) *J. Biol. Chem.* **274,** 236–240
44. Contreras, J. E., Sanchez, H. A., Eugenin, E. A., Speidel, D., Theis, M., Willecke, K., Bukauskas, F. F., Bennett, M. V., and Saez, J. C. (2002) *Proc. Natl. Acad. Sci. U. S. A.* **99,** 495–500
45. Retamal, M. A., Cortes, C. J., Reuss, L., Bennett, M. V., and Saez, J. C. (2006) *Proc. Natl. Acad. Sci. U. S. A.* **103,** 4475–4480
46. Srinivas, M., Hopperstad, M. G., and Spray, D. C. (2001) *Proc. Natl. Acad. Sci. U. S. A.* **98,** 10942–10947